Critical dynamics of the superfluid phase transition: Multiloop calculation of the microscopic model

J. Honkonen [1,*] M. Komarova [2,†] Yu. Molotkov [3,‡] M. Nalimov [2,3,§] and A. Trenogin [2,‖]

[1]*Department of Military Technology, National Defence University, Santahaminantie 2, 00860 Helsinki, Finland*

[2]*Saint-Petersburg State University, 7/9 Universitetskaya Embankment, Saint Petersburg 199034, Russia*

[3]*Bogoliubov Laboratory of Theoretical Physics, Joint Institute for Nuclear Research, 6 Joliot-Curie, Dubna, Moscow Region 141980, Russia*

Results and method of a three-loop renormalization-group calculation in the model of a Bose gas with a local density-density interaction in the formalism of time-dependent Green functions at finite temperature are presented. The results provide support to the recent conjecture [J. Honkonen, M. V. Komarova, Y. G. Molotkov, and M. Y. Nalimov, Nucl. Phys. B **939**, 105 (2019); Y. A. Zhavoronkov, M. V. Komarova, Y. G. Molotkov, M. Y. Nalimov, and J. Honkonen, Theor. Math. Phys. **200**, 1237 (2019)] that the dynamics of the superfluid phase transition is described by a model which belongs to the same universality class as the stochastic model A.

I. INTRODUCTION

Quantum dynamics of boson gas near the Bose-Einstein condensation transition has attracted considerable interest recently. While the static critical behavior of the system is generally believed to belong to the universality class of the *XY* model [or $O(2)$ model] with the corresponding critical exponents, there is no consensus about its dynamic critical behavior and, in particular, the value of the dynamic critical exponent z. Due to soft modes (Goldstone modes) in $O(n)$-symmetric models (related to the second sound in ^{4}He) the scaling theory has fixed the value of the dynamic critical exponent to $z = d/2$ [1,2]. In quantum-statistical models early calculations with the use of temperature Green functions produced a positive correction in the ε expansion to the unrenormalized value $z = 2$ [3], whereas in the $1/n$ expansion the correction was negative and led to values close to the prediction of the scaling theory [4]. These results—as well as a few other microscopic results—were questioned from the point of view of consistency of the exponentiation of logarithmic infrared singularities [2]. Moreover, it is not at all clear that temperature Green functions defined on a finite imaginary time interval are the correct tool for analysis of the long-time asymptotic behavior—after all the correct zero-temperature (i.e., infinite imaginary time) limit leads to the usual zero-temperature Green functions on the whole time axis [5].

The alternative approach based on phenomenological stochastic models of critical dynamics [6] has been prevailing ever since. Therefore, most of the analyses of boson gas systems near the phase transition to superfluid state have been carried out within the stochastic framework. In this case, an estimate of the infrared (i.e., large-scale) behavior of systems is based on the symmetries of the order parameter and the hydrodynamic conservation laws. Physically, it corresponds to the properties of the fields that may be essential in the described asymptotics (e.g., generators of symmetries, the number of components, and space dimension).

The phenomenological models E and F have long been the main candidates for describing the critical dynamics of a Bose gas. According to [6] they contain a set of fields as variables suitable for description of essential hydrodynamic flows. Model F seems more representative, but the data on the experimental and theoretical determination of the critical index α for the specific heat show [7] that the corresponding systems probably degenerate to the simpler model E in the critical region. However, it remained unclear which of the two nontrivial fixed points of the renormalization-group (RG) equation for model E determines the real critical behavior of the boson gas.

A key question not answered by either the E or the F model is the superfluid properties of the Bose gas, e.g., the critical viscosity index, which are closely related to the correct account for dissipation in the corresponding hydrodynamic equations. Recently, it has been proposed to study the stability of the E and F models against the influence of the hydrodynamic velocity field [8–11], and the perturbations by density waves [12]. The RG equation turned out to be sensitive to the activation of hydrodynamic modes, which significantly affect the critical behavior and the exponents. Account of the compressibility of the medium has led to an unexpected conclusion: models E and F are unstable to the density waves, and their IR behavior boils down to that of complex model A, which has a single nontrivial IR stable fixed point of the RG equation.

It should be noted here that the analysis of the significance of hydrodynamic modes and density waves is not trivial and cannot be correctly performed at the stage of constructing a model on the basis of the symmetry. The influence

*juha.honkonen@mil.fi

†m.komarova@spbu.ru

‡saberfull@yandex.ru

§m.nalimov@spbu.ru

‖lastpks@gmail.com

of the corresponding modes is initially associated with formally IR-irrelevant contributions to the action which should be discarded in a straightforward calculation of canonical dimensions. The consistent argument is based on the analysis of propagators and their behavior in the IR region to determine the set of fields and parameters relevant to the critical behavior as well as the combination of physical fields in the order parameter [12]

In a sense, phenomenological constructions acquire completeness if they are corroborated by a microscopic analysis. Indeed, even within a universality class of critical behavior the number of coupling constants and the stability exponents ω may be different. For instance, in models E and F—without activated hydrodynamic modes—an analysis of the time-dependent Green functions at finite temperature (GFFT) of a microscopic model has shown the presence of contributions characteristic of the F model, and also demonstrated the mechanism by which high-frequency modes trigger white noise in the infrared region [13].

Recently, the problem of critical dynamics of a system of nonrelativistic scalar bosons with a local repulsive density-density interaction has been studied with the use of a combination of a field-theoretic RG analysis of the generating functional of GFFT on one hand and a scaling analysis of the effect of density fluctuations in the standard model F on the other [12,14–16]. The use of the grand canonical ensemble in construction of the generating functional of GFFT allows one to avoid problems due to pinch singularities [17]. The remaining singularities characteristics of GFFT were regularized by introduction of auxiliary attenuation of free propagators. The nontrivial behavior of the propagators is an important feature of the problem. On one hand, the regularization of the propagators made it possible to construct a self-consistent diagrammatic expansion. On the other hand, analysis of the Dyson equation of the original model showed that divergences of individual diagrams generate contributions that correspond to hydrodynamic dissipation in the phenomenological model. Discarding the IR-irrelevant part of the action of the regularized model led to an effective multiplicatively renormalizable large-scale model with three coupling constants [14].

Coarse graining leading to the renormalizable model is a process akin to that used in the theory of open quantum systems: to describe the dynamics of a subsystem of a "total" equilibrium Hamiltonian system analyzed in the grand canonical ensemble. In the theory of quantum systems the projection operator technique with assumptions of weakness of correlations between the subsystem and the bath (the rest of the Hamiltonian system) is used to infer the evolution equation of the reduced density operator describing the subsystem [18]. It should also be noted that dissipative Keldysh actions similar to that in [14] had been obtained earlier as the functional solution of the master equation of an open boson system in the Lindblad form with a suitable dissipator [19] as well as

from the solution of the stochastic dissipative Gross-Pitaevskii equation with a suitably chosen noise [20].

Surprisingly, at the only IR stable fixed point below the critical dimension 4 of the perturbatively renormalized effective model [14] the anomalous scaling dimensions—including that of the dynamic exponent z – turned out to be equal to those of the standard model A [6,21]. Contrary to the standard
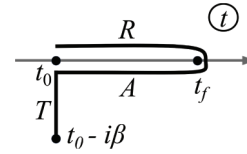

FIG. 1. Schwinger-Keldysh contour in the complex t plane.

model A, however, in the model [14] there are three correction exponents to scaling, which were calculated at the leading nontrivial order in [12,15].

The leading order correction $O(\varepsilon^2)$ of the $\varepsilon = 4 - d$ expansion, however, is not conclusive about the stability of the fixed points in the physical dimension $d = 3$. Therefore, in this paper we report calculation of the correction exponents of the effective model to $O(\varepsilon^3)$. We recall the origin and notation of the model in Sec. II. Section III is devoted to illustration of advantages of the method first proposed in [22] for calculation of dynamic exponents of model A at order $O(\varepsilon^3)$. Here we also quote results of evaluation of renormalization constants. We have calculated 24 two-loop vertex diagrams and 17 three-loop self-energy diagrams; the results are quoted in the Appendix. The contribution $O(\varepsilon^3)$ to one of the correction exponents turned out to change the sign of the exponent at $\varepsilon = 1$ ($d = 3$). In such a situation the ε expansion cannot be trusted without a resummation. In Sec. IV stability of the fixed points is analyzed with the use of the corresponding Borel transform of the values of correction exponents. Summary and conclusions are found in Sec. V.

II. MODEL

In our previous papers [14,15], we proposed a model for calculation of the dynamic critical exponent z for the λ transition. The model was based on the action (in the unit system with $\hbar = 1$)

$$S(\psi, \psi^+) = \int d\mathbf{x} \int_C dt \left[\psi^+ \left(i\partial_t + \frac{\Delta}{2m_0} + \mu \right) \psi \right. $$
$$\left. - \frac{g}{2}(\psi^+ \psi)^2 \right], \quad (1)$$

for quantum boson particles with local repulsive interaction. Here $\psi(t, \mathbf{x})$ and $\psi^+(t, \mathbf{x})$ are complex conjugated fields, m_0 denotes the particle mass, μ denotes the chemical potential, g denotes the coupling constant, and Δ stands for the Laplace operator. We used the formalism of time-dependent Green functions at finite temperature. Thus, the evolution parameter t belongs to the Schwinger-Keldysh contour C (Fig. 1) in the complex t plane [23,24].

To construct the perturbation expansion the fields of (1) were replicated on different parts on the contour by introduction of the fields $\psi_R, \psi_R^+, \psi_A, \psi_A^+, \psi_T$, and ψ_T^+, where the subscripts R, A, and T refer to the corresponding parts of the contour with retarded, advanced, and temperature propagators, respectively.

To regularize the characteristic singularities of this approach on the whole time axis, an attenuation coefficient γ was introduced. We recall that in quantum statistics the

imaginary part of the self-energy function gives rise to a small attenuation coefficient of single-particle excitations [25]. By definition, at the critical point the imaginary part of the self-energy vanishes with vanishing wave number and frequency. Therefore, at the critical point, which we are interested in, the attenuation coefficient in the large-wave-number limit assumes the form αk^2 with the small positive parameter α. It should be noted that $\gamma \propto k^2$ at the critical point is a property of the model. The choice of the coefficient α is a matter of convenience.

After this the reference points of the contour were sent to infinity $t_0 \to -\infty$ and $t_f \to \infty$ to enable the use of the Fourier transform with respect to time. In this limit the contribution of the fields ψ_T and ψ_T^+ of the temperature part of the contour decoupled from the rest and therefore model (1) with attenuation is described in terms of the real-time fields $\psi_R, \psi_R^+, \psi_A,$ and ψ_A^+.

In the grand canonical ensemble all real-time bare propagators of model (1) on the Schwinger-Keldysh contour contain both retarded and advanced parts. For purposes of construction of perturbation theory and the subsequent renormalization it was found convenient to separate the advanced and retarded propagators by introduction of new fields $\xi, \xi^+,$ $\eta,$ and η^+ defined as

$$\xi = \frac{1}{\sqrt{2}}(\psi_R + \psi_A), \quad \eta = \frac{1}{\sqrt{2}}(\psi_R - \psi_A),$$

$$\xi^+ = \frac{1}{\sqrt{2}}(\psi_R^+ + \psi_A^+), \quad \eta^+ = \frac{1}{\sqrt{2}}(\psi_R^+ - \psi_A^+). \quad (2)$$

These new fields are sometimes called the classical and quantum fields [26].

Upon power counting with canonical dimensions corresponding to the parabolic scaling of frequencies and wave numbers and subsequent discarding of the two IR-irrelevant terms of the interaction in (1) an IR effective model was obtained with the following basic action:

$$S = 4\eta\alpha\eta^+ + \eta^+(\partial_t - i\alpha u\Delta - \alpha\Delta)\xi + \xi^+(\partial_t - i\alpha u\Delta + \alpha\Delta)\eta$$

$$+ \frac{i\alpha g_1 \mu^{4-D}}{2}\eta^+\xi^+\xi\xi + \frac{i\alpha g_2 \mu^{4-D}}{2}\eta\xi\xi^+\xi^+ \quad (3)$$

with the scale-setting parameter μ and dimensionless complex charges g_1 and g_2. Integrals are implied in (3) and henceforth notation is streamlined compared to (1).

For the purposes of application of the renormalization group, we consider our model in space dimension $D = 4 - \varepsilon$. The loop theorem of [14] ensures that there are no additional counterterms of structures different from those in (3). This leads to the following form of the renormalized action:

$$S_R = Z_0\eta\eta^+ + \eta^+(Z_1\partial_t - Z_2\Delta)\xi + \xi^+(Z_3\partial_t - Z_4\Delta)\eta$$

$$+ Z_5\mu^{4-D}\eta^+\xi^+\xi\xi + Z_6\mu^{4-D}\eta\xi\xi^+\xi^+ \quad (4)$$

with complex renormalization constants $Z_1, \ldots, Z_6$, each of which is defined as the sum of the coefficient of the field monomial in the basic action (3) and counterterms to it. Moreover, action (3) obeys the symmetry (parameters α and u are positive)

$$S(\eta, \eta^+, \xi, \xi^+, g_1, g_2) = S^*(-\eta^+, -\eta, \xi^+, \xi, g_2^*, g_1^*)$$

$$= S^*(\eta^+, \eta, -\xi^+, -\xi, g_2^*, g_1^*). \quad (5)$$

These conditions impose the following restrictions on the renormalization constants:

$$Z_0 = Z_0^*, Z_1 = Z_3^*, Z_2 = -Z_4^*, Z_5 = -Z_6^* \quad (6)$$

where the change $(g_1, g_2) \to (g_2^*, g_1^*)$ on the right-hand side of the equalities is implied. Furthermore, it is useful to notice that action (3) obeys an additional global gauge symmetry:

$$\xi \to \xi s^{ic}, \quad \xi^+ \to \xi^+ s^{-ic}, \quad \eta \to \eta s^{ic}, \quad \eta^+ \to \eta^+ s^{-ic},$$

where c is some constant. Owing to the global symmetry, we choose the field η to be a real-number function henceforth. Defining renormalization constants of the fields η and ξ and parameters α and u as $\xi = Z_\xi \xi_R$, $\eta = Z_\eta \eta_R$, $u = Z_u u_R$, and $\alpha = Z_\alpha \alpha_R$ we obtain the following system of equations:

$$Z_0 = 4\alpha Z_\eta Z_{\eta^+}, \quad Z_1 = Z_{\eta^+}Z_\xi,$$

$$Z_2 = Z_\alpha Z_{\eta^+} Z_\xi \alpha + i\alpha Z_{\eta^+} Z_u Z_\xi Z_\alpha u,$$

$$Z_5 = \frac{ig_1\alpha}{2} Z_\alpha Z_{g_1} Z_{\eta^+} Z_\xi^2 Z_{\xi^+}. \quad (7)$$

This system of equations can be uniquely resolved only in the hyperspace $g_1 = g_2^*$:

$$Z_{\eta^+} = Z_\eta^*, Z_{\xi^+} = Z_\xi^*, Z_{\eta^+}Z_\xi = Z_1,$$

$$Z_\alpha = \frac{1}{\alpha}\Re(Z_2 Z_1^{-1}), \quad Z_\eta Z_{\eta^+} = \frac{1}{4\alpha}Z_0 Z_\alpha^{-1},$$

$$Z_u = \frac{1}{\alpha u}\Im(Z_2 Z_1^{-1})Z_\alpha^{-1},$$

$$Z_{g_1} = -\frac{i}{2g_1\alpha}Z_5 Z_0 Z_1^{-2}(Z_1^{-1})^* Z_\alpha^{-1}. \quad (8)$$

Our main aim is to verify that the IR-stable fixed point, which was found in [12], is truly stable in higher orders of the perturbation expansion. To accomplish this task we need more information about the β functions and their derivatives calculated at the fixed point. To this end, it is convenient to separate real and imaginary parts of the coupling constants g_1 and g_2: we rewrite the coupling constants as $g_1 = g_r + ig_i$ and $g_2 = g_r - ig_i$ where g_r and g_i are real numbers. In addition to the coupling constants g_r and g_i there is a nonperturbative charge u. In the minimal subtraction scheme used here the corresponding β functions will have the following form:

$$\beta_{g_n} = -\varepsilon g_n + \varepsilon g_n \sum_{m=r,i} g_m \frac{\partial[Z_{g_n}]}{\partial g_m},$$

$$\beta_u = \varepsilon u \sum_{m=r,i} g_m \frac{\partial[Z_u]}{\partial g_m} \quad (9)$$

where $n = r, i, u$ is the nonperturbative charge and $[Z]$ denotes the residue of the simple pole in the Laurent expansion in ε of the corresponding renormalization constant.

III. CALCULATION

We will consider model (3) in space dimension $4 - \varepsilon$ with dimensional regularization in the minimal subtraction scheme $\overline{\text{MS}}$ (for details, see, e.g., [7]). The three-loop contribution will be calculated using the bare propagators of (3) of the form [12,14]

$$\langle\eta(t,\mathbf{k})\xi^+(t',-\mathbf{k})\rangle_0 = -\theta(t'-t)e^{-i\alpha u k^2(t-t')-\alpha k^2|t-t'|},$$

$$\langle\eta(t,\mathbf{k})\eta^+(t',-\mathbf{k})\rangle_0 = 0,$$

$$\langle\xi(t,\mathbf{k})\eta^+(t',-\mathbf{k})\rangle_0 = \theta(t-t')e^{-i\alpha u k^2(t-t')-\alpha k^2|t-t'|},$$

$$\langle\xi(t,\mathbf{k})\xi^+(t',-\mathbf{k})\rangle_0 = \frac{2}{k^2}\, e^{-i\alpha u k^2(t-t')-\alpha k^2|t-t'|}. \tag{10}$$

As explicitly stated in (9), in the $\overline{\text{MS}}$ scheme only residues of simple poles in ε of the counterterms contribute to the coefficient functions of the RG equations. Therefore, the relevant part of renormalization constants (7) can be presented in the form

$$Z_0(g_1,g_2,u) = 4\alpha - \frac{\alpha g_1 g_2 M_1(u)}{2\times 16^2\pi^4\varepsilon} + \frac{(-i)g_1 g_2^2\alpha Q_{10}(u)}{16^3\pi^6\varepsilon} + \frac{(-i)g_1^2 g_2\alpha Q_{11}(u)}{16^3\pi^6\varepsilon},$$

$$Z_1(g_1,g_2,u) = 1 + \frac{g_1^2 M_3(u)}{16^2\pi^4\varepsilon} - \frac{g_1 g_2 M_2(u)}{2\times 16^2\pi^4\varepsilon} + \frac{(-i)g_1^3 Q_4(u)}{16^3\pi^6\varepsilon} + \frac{(-i)g_1^2 g_2 Q_5(u)}{16^3\pi^6\varepsilon} + \frac{(-i)g_1 g_2^2 Q_6(u)}{16^3\pi^6\varepsilon},$$

$$Z_2(g_1,g_2,u) = (1+iu)\alpha + \frac{g_1^2\alpha(2-iu)}{16^2\pi^4(3-iu)\varepsilon} - \frac{g_1 g_2\alpha(1-iu)}{16^2\pi^4(3-iu)\varepsilon} + \frac{(-i)g_1^3\alpha Q_7(u)}{16^3\pi^6\varepsilon} + \frac{(-i)g_1^2 g_2\alpha Q_8(u)}{16^3\pi^6\varepsilon} + \frac{(-i)g_1 g_2^2\alpha Q_9(u)}{16^3\pi^6\varepsilon},$$

$$Z_5(g_1,g_2,u) = \frac{ig_1\alpha}{2} - \frac{g_1^2\alpha}{16(1+iu)\pi^2\varepsilon} - \frac{g_1^2\alpha}{8\pi^2\varepsilon} + \frac{g_1 g_2\alpha}{8\pi^2\varepsilon} - \frac{ig_1^3\alpha}{64\pi^4\varepsilon}Q_1(u) - \frac{ig_1^2 g_2\alpha}{128\pi^4\varepsilon}Q_2(u) - \frac{ig_1 g_2^2\alpha}{128\pi^4\varepsilon}Q_3(u), \tag{11}$$

where functions $M_i(u)$ of the nonperturbative coupling constant u were calculated in [14]:

$$M_1 = \frac{A + 3B - \pi u - 2u\arctan C_-}{u^2 + 1},$$

$$M_2 = \frac{(u-i)^2(2i\arctan(2C_+) - \pi i - A - B)}{(u^2+1)^2},$$

$$M_3 = \frac{(u+i)^2(B - 2i\arctan(u/3))}{(u^2+1)^2},$$

$$A = \ln(u^2+1), \;\; B = \ln\left(\frac{u^2+9}{16}\right), \;\; C_\pm = \frac{u^2\pm 3}{4u}.$$

In the present model—like in model A—the leading order (measured in the expansion parameter ε) of fluctuation corrections to β_{g_1} and β_{g_2} is given by one-loop vertex graphs, whereas corrections to β_u are inferred from two-loop self-energy graphs. Here, we are calculating the next-to-leading corrections, for which it is sufficient to calculate three-loop self-energy graphs (listed in Tables I and II of the Appendix) and two-loop vertex graphs (listed in Table III of the Appendix).

The two- and three-loop coefficient functions Q_i can be calculated with the aid of the sector decomposition method [27]. However, a more subtle approach will be used here. Apparently, this approach was first applied in the three-loop calculation of the dynamic critical exponents of the model A in [22] and we briefly review the main concept here.

At the third order of the perturbation theory there are three topological types of diagrams, depicted below:

It is easily seen that the first type of these diagrams is a product of two diagrams of the first order. Therefore, these diagrams

are totally irrelevant to calculation of the β and γ functions, because upon subtraction of contributions brought about by divergent subgraphs no simple poles in ε are left and thus these graphs do not contribute to the β and γ functions of the RG equation [7].

A. Method of calculation

Let us describe the method of calculation in more detail. The origin of the approach lies in the possibility to perform in a closed form the Fourier transform of the function

$$\frac{\theta(t - t_2)}{(t - t_2)^c}\exp[-\mathbf{p}^2(t - t_2)c_1]$$

both with respect to $\mathbf{p}$ to arrive at a function of $(\mathbf{x} - \mathbf{x}_2)$ and with respect to t to obtain a function of ω. Comparison of these results leads to the following explicit expression for the Fourier transform from variables $(t,\mathbf{x})$ to $(\omega,\mathbf{p})$. For Re $c_1 > 0$ the result for arbitrary A, a, and Re $b1 > 0$ is

$$A\frac{\theta(t-t_2)}{(t-t_2)^a}\exp\left[-\frac{(\mathbf{x}-\mathbf{x}_2)^2}{t-t_2}b\right]$$

$$\xrightarrow{\text{Fourier}} A\left(\frac{\pi}{b}\right)^{D/2}\frac{\Gamma\left(\frac{D}{2}+1-a\right)}{\left(\frac{p^2}{4b}-i\omega\right)^{\frac{D}{2}+1-a}},$$

$$A\frac{\theta(t_2-t)}{(t_2-t)^a}\exp\left(-\frac{(\mathbf{x}-\mathbf{x}_2)^2}{t_2-t}b_1\right)$$

$$\xrightarrow{\text{Fourier}} A\left(\frac{\pi}{b}\right)^{\frac{D}{2}}\frac{\Gamma\left(\frac{D}{2}+1-a_1\right)}{\left(\frac{p^2}{4b}+i\omega\right)^{\frac{D}{2}+1-a}}, \tag{12}$$

where D is the dimension of space. Propagator lines similar to those in (12) will be called "standard form" lines. The loop diagrams with lines in the form of the right-hand side of (12) can be simply calculated. After the inverse Fourier transform

of all lines into the $(t, \mathbf{x})$ presentation expressions in the form of the left-hand side of (12) must be multiplied. It is essential that the result is of the standard form of the left-hand side of (12) with the product of A-type factors and sum of a-type and b-type arguments. It can be readily transformed to the $(\omega, \mathbf{p})$ representation by the procedure (12), which leads to the standard form as well.

B. Convolution of lines

With the use of (12) propagator lines are cast into the $(\omega, \mathbf{p})$ representation in which the convolution of two arbitrary lines of standard form is transformed to a simple product of the form

$$\frac{A}{\left(\frac{p^2}{4b} - i\omega\right)^a} \frac{A_1}{\left(\frac{p^2}{4b_1} - i\omega\right)^{a_1}}$$

or

$$\frac{A}{\left(\frac{p^2}{4b} - i\omega\right)^a} \frac{A_1}{\left(\frac{p^2}{4b_1} + i\omega\right)^{a_1}},$$

depending on arguments of the θ functions in propagators. The Feynman identity

$$\frac{1}{B^a B_1^{a_1}} = \frac{\Gamma(a + a_1)}{\Gamma(a)\Gamma(a_1)} \int_0^1 dz \int_0^1 dz_1 \frac{\delta(z + z_1 - 1) z^{a-1} z_1^{a_1-1}}{[Bz + B_1 z_1]^{a+a_1}}$$

produces

$$\frac{AA_1 \Gamma(a + a_1)}{\Gamma(a)\Gamma(a_1)} \int_0^1 dz_1 \frac{(1 - z_1)^{a-1} z_1^{a_1-1}}{\left[\frac{p^2}{4b}(1 - z_1) + z_1 \frac{p^2}{4b_1} - i\omega\right]^{a+a_1}}$$

in the first case or

$$\frac{AA_1 \Gamma(a + a_1)}{\Gamma(a)\Gamma(a_1)} \int_0^1 dz \frac{(z)^{a-1}(1 - z)^{a_1-1}}{\left[\frac{p^2}{4b}z + (1 - z)\frac{p^2}{4b_1} + i\omega(1 - 2z)\right]^{a+a_1}}$$

in the second.

The first expression is of the standard form. To transform to the standard form the second expression the integral over z is split in a sum of two, the first one over $0 < z < 1/2$ and the second over $1/2 < z < 1$. These parts contribute to different step functions in the $(t, \mathbf{x})$ representation. It is convenient to scale the z variables to obtain integrals in new variables z_1 in the limits $0 < z_1 < 1$.

After the inverse Fourier transform the convolution integrals over $(t_1, \mathbf{x}_1)$ may be expressed as

$$\int d\mathbf{x}_1 dt_1 A_1 \frac{\theta(t - t_1)}{(t - t_1)^{a_1}} \exp\left(-\frac{(x - x_1)^2}{t - t_1} b_1\right) A_2 \frac{\theta(t_1 - t_2)}{(t_1 - t_2)^{a_2}} \exp\left(-\frac{(x_1 - x_2)^2}{t_1 - t_2} b_2\right)$$

$$= A_1 A_2 \left(\frac{\pi}{b_1 b_2}\right)^{\frac{D}{2}} \int_0^1 dz_1 z_1^{\frac{D}{2} - a_1} (1 - z_1)^{\frac{D}{2} - a_2} \left(\frac{z_1}{b_1} + \frac{1 - z_1}{b_2}\right)^{-\frac{D}{2}} \frac{\theta(t - t_2)}{(t - t_2)^{a_1 + a_2 - \frac{D}{2} - 1}} \exp\left(-\frac{(x - x_2)^2}{t - t_2} \left(\frac{z_1}{b_1} + \frac{1 - z_1}{b_2}\right)^{-1}\right),$$

(13)

$$\int dx_1 dt_1 A_1 \frac{\theta(t - t_1)}{(t - t_1)^{a_1}} \exp\left(-\frac{(x - x_1)^2}{t - t_1} b_1\right) A_2 \frac{\theta(t_2 - t_1)}{(t_2 - t_1)^{a_2}} \exp\left(-\frac{(x_1 - x_2)^2}{t_2 - t_1} b_2\right)$$

$$= \frac{A_1 A_2}{2^{\frac{D}{2} + 1 - a_1 - a_2}} \left(\frac{\pi}{b_1 b_2}\right)^{\frac{D}{2}} \int_0^1 dz_1 z_1^{a_1 + a_2 - \frac{D}{2} - 2} \left[(1 - z_1)^{\frac{D}{2} - a_1}(1 + z_1)^{\frac{D}{2} - a_2} \left(\frac{1 - z_1}{b_1} + \frac{1 + z_1}{b_2}\right)^{-\frac{D}{2}} \frac{\theta(t_2 - t)}{(t_2 - t)^{a_1 + a_2 - \frac{D}{2} - 1}}\right.$$

$$\times \exp\left(-2z_1 \frac{(x - x_2)^2}{t_2 - t} \left(\frac{1 - z_1}{b_1} + \frac{1 + z_1}{b_2}\right)^{-1}\right) + (1 + z_1)^{\frac{D}{2} - a_1}(1 - z_1)^{\frac{D}{2} - a_2} \left(\frac{1 + z_1}{b_1} + \frac{1 - z_1}{b_2}\right)^{-\frac{D}{2}}$$

$$\times \frac{\theta(t - t_2)}{(t - t_2)^{a_1 + a_2 - \frac{D}{2} - 1}} \exp\left(-2z_1 \frac{(x - x_2)^2}{t - t_2} \left(\frac{1 + z_1}{b_1} + \frac{1 - z_1}{b_2}\right)^{-1}\right)\right],$$

(14)

$$\int dx_1 dt_1 A_1 \frac{\theta(t_1 - t)}{(t_1 - t)^{a_1}} \exp\left(-\frac{(x - x_1)^2}{t_1 - t} b_1\right) A_2 \frac{\theta(t_1 - t_2)}{(t_1 - t_2)^{a_2}} \exp\left(-\frac{(x_1 - x_2)^2}{t_1 - t_2} b_2\right)$$

$$= \frac{A_1 A_2}{2^{\frac{D}{2} + 1 - a_1 - a_2}} \left(\frac{\pi}{b_1 b_2}\right)^{\frac{D}{2}} \int_0^1 dz_1 z_1^{a_1 + a_2 - \frac{D}{2} - 2} \left[(1 + z_1)^{\frac{D}{2} - a_1}(1 - z_1)^{\frac{D}{2} - a_2} \left(\frac{1 + z_1}{b_1} + \frac{1 - z_1}{b_2}\right)^{-\frac{D}{2}}\right.$$

$$\times \frac{\theta(t_2 - t)}{(t_2 - t)^{a_1 + a_2 - \frac{D}{2} - 1}} \exp\left(-2z_1 \frac{(x - x_2)^2}{t_2 - t} \left(\frac{1 + z_1}{b_1} + \frac{1 - u_1}{b_2}\right)^{-1}\right) + (1 - z_1)^{\frac{D}{2} - a_1}(1 + z_1)^{\frac{D}{2} - a_2}$$

$$\times \left(\frac{1 - z_1}{b_1} + \frac{1 + z_1}{b_2}\right)^{-\frac{D}{2}} \frac{\theta(t - t_2)}{(t - t_2)^{a_1 + a_2 - \frac{D}{2} - 1}} \exp\left(-2z_1 \frac{(x - x_2)^2}{t - t_2} \left(\frac{1 - z_1}{b_1} + \frac{1 + z_1}{b_2}\right)^{-1}\right)\right],$$

(15)

$$\int dx_1 dt_1 A_1 \frac{\theta(t_1 - t)}{(t_1 - t)^{a_1}} \exp\left(-\frac{(x - x_1)^2}{t_1 - t} b_1\right) A_2 \frac{\theta(t_2 - t_1)}{(t_2 - t_1)^{a_2}} \exp\left(-\frac{(x_1 - x_2)^2}{t_2 - t_1} b_2\right)$$

$$= A_1 A_2 \left(\frac{\pi}{b_1 b_2}\right)^{\frac{D}{2}} \int_0^1 dz_1 z_1^{\frac{D}{2} - a_1} (1 - z_1)^{\frac{D}{2} - a_2} \left(\frac{z_1}{b_1} + \frac{1 - z_1}{b_2}\right)^{-\frac{D}{2}} \frac{\theta(t_2 - t)}{(t_2 - t)^{a_1 + a_2 - \frac{D}{2} - 1}} \exp\left(-\frac{(x - x_2)^2}{t_2 - t} \left(\frac{z_1}{b_1} + \frac{1 - z_1}{b_2}\right)^{-1}\right).$$

It is essential that the expressions obtained have the standard form or are the sum of the standard form lines. Therefore, these expressions can be used in the subsequent steps in the method described here.

C. Example

Here, we demonstrate the method of calculation by evaluating a diagram of the second type:

(16)
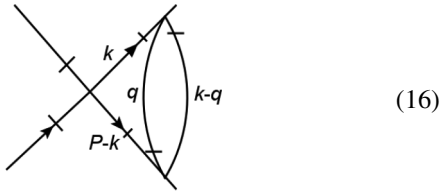
To start calculation all propagators (10) must be presented in the standard form. Three of them have already the necessary form. The remaining one should be transformed. To deal with the modulus we should separate positive and negative values of t with the aid of the Heaviside step function:

$$\langle \xi(t, \mathbf{k}) \xi^+(t', -\mathbf{k}) \rangle_0 = \frac{2e^{-i\alpha u k^2 (t - t') - \alpha k^2 |t - t'|}}{k^2}$$

$$= \frac{2e^{-i\alpha u k^2 (t - t') - \alpha k^2 (t - t')}}{k^2} \theta(t - t')$$

$$+ \frac{2e^{-i\alpha u k^2 (t - t') + \alpha k^2 (t - t')}}{k^2} \theta(t' - t).$$

(17)

The next step is to transform both terms. They have common structure, therefore we will describe transformation only for one of them; the other can be obtained in a similar way:

$$\frac{2e^{-i\alpha u k^2 t - \alpha k^2 t}}{k^2} \theta(t) = \int_1^\infty ds \, 2\theta(t) e^{-k^2 s t \alpha(iu + 1)} t \alpha(iu + 1)$$

$$= \int_0^1 \frac{ds}{s^2} 2\theta(t) e^{-\frac{k^2 t \alpha(iu + 1)}{s}} t \alpha(iu + 1) \xrightarrow{\text{Fourier}}$$

$$\times \frac{2\theta(t)}{(2\pi)^D} \int_0^1 \frac{ds}{s^{2 - \frac{D}{2}}} e^{-\frac{x^2 s}{4t\alpha(iu + 1)}} \pi^{\frac{D}{2}} t^{1 - \frac{D}{2}}$$

$$\times \alpha^{1 - \frac{D}{2}} (1 + iu)^{1 - \frac{D}{2}}.$$

(18)

Applying the Fourier transform to other propagators in (10) we arrive at a set of standard form propagators in the $(t, \mathbf{x})$ representation. Diagram (16) contributes to the renormalization constant Z_5. To calculate this contribution we put the momentum and frequency of the external line in the upper

right corner equal to zero. Then we have to calculate

(19)
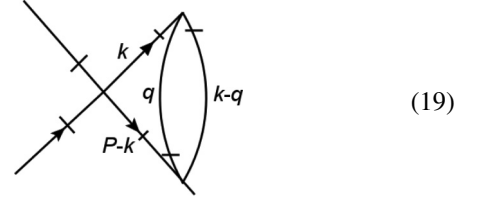
First, we multiply in the $(t, \mathbf{x})$ presentation the lines in the right loop marked by $q, k - q$ in (19). The result is in the standard form, so that using (15) we calculate its convolution with the upper $\langle \xi \eta^+ \rangle_0$ line marked by k. The result of the convolution is a sum of lines in the standard form. Every one of these lines is simply multiplied by the lower line $\langle \xi \eta^+ \rangle_0$ marked by $p - k$.

After the transform to the $(\omega, \mathbf{p})$ representation with the use of (12) we obtain the result in the form of integrals over two variables similar to that over s in (18) and over z in (15). The Γ function due to Fourier transform contains the leading pole in ε. The second pole in ε can be simply extracted from the integral over z. The remaining integrals are readily calculated analytically or numerically.

This technique allows us to extract a residue of corresponding expressions almost directly for all the above-mentioned types of diagrams. Moreover, in some cases this approach can be used to obtain closed-form expressions for the diagrams.

D. Results of calculations

At the IR stable fixed point found in [12] the nonperturbative coupling constant u is equal to zero. To prove the stability of this point in the next perturbation order only values of functions $Q_i(u)$ and their derivatives with respect to u at $u = 0$ are required. The result of calculation of the first three functions is

$$Q_1(0) = -\log\left(\frac{4}{3}\right) - 3, \quad Q_2(0) = -7 + 18 \coth^{-1}(7),$$

$$Q_3(0) = 3 - 14 \coth^{-1}(7),$$

$$\left.\frac{\partial Q_1(u)}{\partial u}\right|_{u=0} = \frac{i(72 \coth^{-1}(7) - 25)}{6},$$

$$\left.\frac{\partial Q_2(u)}{\partial u}\right|_{u=0} = \frac{2i(2 + 9 \coth^{-1}(7))}{3},$$

$$\left.\frac{\partial Q_3(u)}{\partial u}\right|_{u=0} = \frac{i(11 - 114 \coth^{-1}(7))}{3}.$$

(20)

Expressions for $Q_4, \ldots, Q_{10}$ are more complicated and include the dilogarithm $\text{Li}_2(1/9)$ (also known as Spence's

function). We calculated them with the use of the method described in Sec. III with the result

$$Q_4(0) = -\frac{40\pi^2}{9} + \frac{4B_1}{3} - 8\left(\log\left(\frac{4}{3}\right) - 26\log^2(2)\right)$$
$$+ \frac{4}{3}\log(3)(49\log(3) - 160\log(2)),$$

$$Q_5(0) = \frac{B_2}{3} + \frac{8\pi^2}{3} - \frac{4}{3}\log(2)(23 + 83\log(2))$$
$$+ \frac{1}{3}(54 + 296\log(2) - 79\log(3))\log(3),$$

$$Q_6(0) = \frac{B_3}{3} - \frac{35\pi^2}{18} + \frac{2}{3}\log(2)(163\log(2) - 58)$$
$$+ \frac{1}{3}\log(3)(66 - 344\log(2) + 97\log(3)),$$

$$Q_7(0) = -\frac{32\text{Li}_2\left(\frac{1}{4}\right)}{3} - \frac{64\text{Li}_2\left(\frac{1}{3}\right)}{3} - \frac{2}{3} + \frac{16\pi^2}{9}$$
$$- \frac{64\log^2(2)}{3} + \frac{64}{3}\log(3)\coth^{-1}(7),$$

$$Q_8(0) = -\frac{16\pi^2}{9} + 64\log^2(2) - \frac{4}{9}\log(2)(83 + 144\log(3))$$
$$+ \frac{1}{6}(B_4 + 7 + 4\log(3)(33 + 32\log(3))),$$

$$Q_9(0) = \frac{1}{18}(-1 + 16\pi^2 - 8\log(2)(73 + 48\coth^{-1}(5)))$$
$$+ \frac{1}{18}\left(-192\text{Li}_2\left(\frac{1}{4}\right) - 96\text{Li}_2\left(\frac{1}{3}\right) + 356\log(3)\right),$$

$$Q_{10}(0) = -Q_{11}(0) = \frac{20\pi^2}{3} - \frac{160\text{Li}_2\left(\frac{3}{4}\right)}{3} + \frac{20}{3}\log\left(\frac{4}{3}\right)$$
$$\times (-6 + 26\log(2) - 21\log(3)), \quad (21)$$

where

$$B_1 = -4\text{Li}_2(1/16) + 6\text{Li}_2(1/9) - 4\text{Li}_2(1/6)$$
$$+ 34\text{Li}_2(1/4) + 12\text{Li}_2(3/8) + 8\text{Li}_2(4/9) + 4\text{Li}_2(2/3),$$
$$B_2 = 4(4\text{Li}_2(1/16) - \text{Li}_2(1/9) + 4\text{Li}_2(1/6)$$
$$- 33\text{Li}_2(1/4) - 12\text{Li}_2(3/8) - 8\text{Li}_2(4/9) + 9\text{Li}_2(2/3)),$$
$$B_3 = -8\text{Li}_2(1/16) + 12\text{Li}_2(1/9) - 8\text{Li}_2(1/6)$$
$$+ 29\text{Li}_2(1/4) + 8(\text{Li}_2(1/3) + 3\text{Li}_2(3/8) + 2\text{Li}_2(4/9)),$$
$$B_4 = 32\text{Li}_2\left(\frac{1}{4}\right) + 160\text{Li}_2\left(\frac{1}{3}\right). \quad (22)$$

The derivatives of Q_i with respect to u at $u = 0$ were evaluated in a similar way and their closed-form expressions also include dilogarithms:

$$\partial_u Q_4(u)\big|_{u=0} = -\frac{4}{3}i(368\log(2) - 89\log(3))\log(3)$$
$$- \frac{32}{3}i(\log(2)(49\log(2) - 12) + \log(729))$$
$$+ \frac{4}{9}i(-3C_1 + 19\pi^2 - 18),$$

$$\partial_u Q_5(u)\big|_{u=0} = \frac{1}{9}i(C_2 + \pi^2 - 87(\log^2(3) + \log(9)))$$
$$- \frac{4}{9}i\log(2)(-83 + 66\log(2) - 87\log(3)),$$

$$\partial_u Q_6(u)\big|_{u=0} = \frac{2}{9}i(319\log(3) + (576\log(2) - 299)\log(4))$$
$$- \frac{1}{9}i(C_3 + 46\pi^2 + 21(136\log(2)$$
$$- 47\log(3))\log(3)),$$

$$\partial_u Q_7(u)\big|_{u=0} = -\frac{1}{9}i(C_4 + 8\pi^2 + 29)$$
$$- \frac{4}{9}i\log(2)(-101 + 312\log(2) - 288\log(3)),$$

$$\partial_u Q_8(u)\big|_{u=0} = -\frac{2}{9}i(C_5 + 8\log(3)(17 + \log(729))) + \frac{2}{27}i$$
$$\times (3 + 24\pi^2 + 16\log(2)(41 + 63\coth^{-1}(5))),$$

$$\partial_u Q_9(u)\big|_{u=0} = \frac{1}{54}i(C_6 + 72\pi^2 + 195) + \frac{2}{27}i\log(2)$$
$$\times (-665 + 1944\log(2) - 1728\log(3)), \quad (23)$$

where

$$C_1 = -10\text{Li}_2(1/9) + 32\text{Li}_2(2/3) + 28\text{Li}_2(3/4),$$
$$C_2 = 84\text{Li}_2(-2) - 18\text{Li}_2(1/9) + 114\text{Li}_2(1/4),$$
$$C_3 = -6(5\text{Li}_2(1/9) - 44\text{Li}_2(1/4)$$
$$+ 94\text{Li}_2(2/3) + \text{Li}_2(3/4) + 10),$$
$$C_4 = 48\text{Li}_2(1/4) - 96\text{Li}_2(2/3)$$
$$+ 101\log(9) + 120\log(3)\log(9),$$
$$C_5 = 72\text{Li}_2(-1/3) + 72\text{Li}_2(2/3) + 36\text{Li}_2(3/4),$$
$$C_6 = 432\text{Li}_2(1/4) - 864\text{Li}_2(2/3)$$
$$+ (697 + 648\log(3))\log(9).$$

With the use of these expressions, the RG functions β_{g_r}, β_{g_i}, and β_u can be directly evaluated. However, their closed-form expressions are too lengthy to include here and we therefore quote them in numerical form:

$$\beta_{g_r}(g_r, g_i, 0) = 0.004\,335\,38 g_i^2 g_r - 0.075\,990\,9 g_i g_r$$
$$- \varepsilon g_r + 0.000\,271\,762 g_r^3,$$

$$\beta_{g_i}(g_r, g_i, 0) = -0.001\,336\,72 g_i g_r^2 - \varepsilon g_i + 0.002\,726\,9 g_i^3$$
$$- 0.063\,325\,7 g_i^2 + 0.012\,665\,1 g_r^2,$$

$$\beta_u(g_r, g_i, 0) = -0.000\,077\,646 g_i g_r + 2.767\,327\,16$$
$$\times 10^{-6} g_i^2 g_r + 1.800\,921\,45 \times 10^{-7} g_r^3. \quad (24)$$

The nonperturbative coupling constant u has been set equal to zero in (24), because at the only nontrivial perturbative fixed point it assumes the value $u_* = 0$ [12].

IV. BOREL TRANSFORM

Let us briefly recall the results of the RG analysis at the leading order of the ε expansion [12,16]: Contrary to the case of stochastic models E and F, there are only three fixed points for the set of the three equations $\beta_{g_r}(g_r, g_i, u) = 0$, $\beta_{g_i}(g_r, g_i, u) = 0$, and $\beta_u(g_r, g_i, u) = 0$. Apart from the trivial fixed point $g_{r*} = g_{i*} = 0$ with arbitrary u_* (IR unstable at $d < 4$), there is the saddle point $g_i = -2\pi^2\varepsilon$, $1/u = 0$ with

arbitrary g_r, and the only IR stable (at $d < 4$) fixed point $g_{r*} = 0$, $g_{i*} = -8\pi^2\epsilon/5$, $u_* = 0$, the stability of which is further explored in the present analysis.

The connection between the critical behavior of the present model and model A can be illustrated as follows. Let us define new two-component variables ϕ (real) and ϕ' (imaginary) as $\phi_1' = \eta^+ - \eta$, $\phi_2' = i(\eta^+ + \eta)$, $\phi_1 = (\xi^+ + \xi)/2$, and $\phi_2 = i(\xi^+ - \xi)/2$. Then the action (3) at the only IR-stable fixed point (with imaginary charge $g = ig_{i*}$) becomes

$$S_* = \alpha\phi'^2 + \phi'\left[-\partial_t\phi + \alpha\left(\Delta\phi + \frac{g_{i*}}{2}\phi^3\right)\right]. \quad (25)$$

This expression coincides with the De Dominicis–Janssen action [28,29] of the stochastic two-component model A [7] up to notation. Moreover, the sign of g_{i*} in (25) matches that in model A [7].

It was shown in [12] that the coupling constants g_r and u are equal to zero at the IR stable fixed point. Therefore, to obtain the fixed point in the next-to-leading-order equation $\beta_{g_i}(0, g_i, 0) = 0$ should be solved. As a result, the fixed point has the following form:

$$g_{i*} = -\frac{8\pi^2\varepsilon}{5} + \frac{136\pi^2\varepsilon^2}{125}. \quad (26)$$

The character of the fixed point is determined by the eigenvalues of the ω matrix consisting of derivatives of the β functions with respect to coupling constants calculated at the fixed point. At an IR stable fixed point all eigenvalues of the matrix

$$\omega = \begin{pmatrix} \frac{\partial\beta_{g_r}}{\partial g_r} & \frac{\partial\beta_{g_r}}{\partial g_i} & \frac{\partial\beta_{g_r}}{\partial u} \\ \frac{\partial\beta_{g_i}}{\partial g_r} & \frac{\partial\beta_{g_i}}{\partial g_i} & \frac{\partial\beta_{g_i}}{\partial u} \\ \frac{\partial\beta_u}{\partial g_r} & \frac{\partial\beta_u}{\partial g_i} & \frac{\partial\beta_u}{\partial u} \end{pmatrix} \quad (27)$$

are strictly positive. Evaluation of the eigenvalues of the ω matrix leads to the following answers:

$$\varepsilon + 0.68\varepsilon^2,$$
$$0.2\varepsilon + 0.245\,739\varepsilon^2,$$
$$0.023\,014\,6\varepsilon^2 - 0.025\,833\,6\varepsilon^3. \quad (28)$$

The coefficient of ε^2 of the leading-order contribution to the third eigenvalue in (28) is a small number, therefore at the physical value of the expansion parameter $\varepsilon = 1$ it is highly sensitive to corrections of higher order. The present next-to-leading-order calculation was undertaken in order to verify the conclusion about stability of the fixed point at hand. It is easy to see that in three dimensions ($\varepsilon = 1$) the third eigenvalue in (28) has a negative sign. Moreover, for this eigenvalue the next-to-leading order is larger then the leading one. In such a situation it is difficult to use directly the perturbation expansion. Usually in the quantum-field perturbation series values a few first terms decrease. In that case the sum of the leading terms can be considered as a correct estimate of the number inferred from the asymptotic series.

In the present case a series resummation is necessary. Usually the quantum field perturbation series resummation is based on known high-order asymptotes (HOAs) of the series. In the GFFT formalism used here the HOA has not been

investigated yet. For our purposes, however, it is not needed in the full size. Here, we calculate the ω exponents at the fixed point only. All calculations were performed for $g_r = u = 0$. Therefore, we need in fact to analyze some Green functions in the dynamical model A. The HOAs of the perturbation series in this model are known [30,31]. These results may be used for the resummation of the present ω exponents.

According to [30,31] the fixed point coordinates and ω exponents of $g_r = u = 0$ behavior are of the form

$$q = \sum_{N \geqslant 0} q_N \varepsilon^N \quad (29)$$

with the HOA

$$q_N = C_q N!(-a)^N N^{b_q}(1 + O(1/N)). \quad (30)$$

The right side of relation (30) is an asymptotic estimate of the coefficient in the Nth order of perturbation theory, the parameters of which are

$$a = \frac{3}{10}, \quad b_{\omega_3} = 4, \quad b_{\omega_1} = b_{\omega_2} = 5. \quad (31)$$

Let us recall the main features of the Borel resummation [32,33]. For q (29) with HOA (30) the Borel transform is defined by the formulas

$$q(\varepsilon) = \int_0^{+\infty} dt\, t^b e^{-t} B(\varepsilon t), \quad B(x) = \sum_{k \geqslant 0} B_k x^k,$$
$$B_k = \frac{q_k}{\Gamma(k + b + 1)}, \quad (32)$$

where b is an arbitrary parameter.

The related conformal mapping has usually the form [32,33]

$$v(x) = \frac{\sqrt{1 + ax} - 1}{\sqrt{1 + ax} + 1} \quad \Leftrightarrow \quad x(v) = \frac{4v}{a(v-1)^2}. \quad (33)$$

The integration contour here belongs to a convergence circle, the point $x = -1/a$ is mapped to $v = -1$, and the infinity point goes to $v = 1$. Small values of x in (33) correspond to small v. Therefore, the series (32) can be rewritten in terms of the v variable:

$$B(x) = \sum_{n \geqslant 0} x^n B_n \quad \longrightarrow \quad B(u) = \sum_{n \geqslant 0} v^n V_n,$$

where

$$V_0 = B_0, \quad V_n = \sum_{m=1}^{n} B_m(4/a)^m C_{n+m-1}^{n-m}, \quad n \geqslant 1. \quad (34)$$

Correspondingly conformal-Borel transform of the Q function has the form

$$q(\varepsilon) = \sum_{k \geqslant 0} V_k \int_0^{+\infty} dt\, t^b e^{-t} (v(\varepsilon t))^k. \quad (35)$$

In [32] the parameter b was chosen in accordance with the condition $b \geqslant b_z + 1.5$. Such a choice allows one to "weaken" the singularity of the Borel image (32) at the point $x = -1/a$. Using conformal-Borel transform in our case with $b = b_z + 1.5$ we obtain ($\varepsilon = 1$)

$$\omega_1 = 0.211\,669\,753\,1,$$

$$\omega_2 = 1.078\,902\,843,$$

$$\omega_3 = 0.003\,120\,033\,385. \tag{36}$$

Numerical results of resummation weakly depend on the scheme used. According to [34], conformal-Borel transform yields the most accurate figures. Taking into account two orders of the perturbation expansion it is not plausible to ensure high accuracy of the result obtained. However, here only the signs of the ω exponents are essential. All three eigenvalues are strictly positive now. It is worthwhile to note that the next perturbation order must increase this result due to the sign alternation of the series. This confirms that in the third order of the perturbation theory the fixed point investigated is IR stable.

V. CONCLUSION

With the use of three-loop calculation in the model of a Bose gas with a local density-density interaction in the formalism of the time-dependent Green functions at finite temperature we have corroborated our previous conjecture [12,14] that the dynamics of the superfluid phase transition is described by a model which belongs to the same class of universality as the stochastic model A. This is a main physical result of the paper.

We have also demonstrated the usefulness of the slightly developed method of calculation of dynamical diagrams in the $(t, \mathbf{x})$ representation proposed in [22]. Using this approach we have obtained analytical results for two- and three-loop graphs. The propagators in our model are similar to those in the stochastic model F which is more general and difficult than the widely investigated model E. The renormalization group calculations in model E at the same order in loop as in the present paper were performed in [35–37] with different results. The definite result was obtained only recently in [38]. The $(t, \mathbf{x})$ approach can simplify essentially multiloop calculations in an arbitrary dynamic model.

In addition to the dynamics near the λ point description in the GFFT formalism a stochastic model was put forward in [12,16] which produces similar results in the description of the critical behavior. The stochastic model is a model of classical fields, however, and it includes quantities like velocity and viscosity as classical variables. Using stochastic equations of this model it is possible to calculate the critical dimension of the viscosity and show how viscosity tends to zero in the superfluid phase transition. We hope to publish the results of the investigation soon.

ACKNOWLEDGMENTS

APPENDIX: FEYNMAN DIAGRAMS

In this Appendix we present the results of calculation of two- and three-loop diagrams. Unfortunately, we have not obtained analytic results for diagrams for arbitrary u, and the

expressions from numerical calculations of graphs with $u \neq 0$ are too large. Therefore, we present here expressions at $u = 0$ for graphs and their derivatives with respect to u. These results can be useful for investigations of other models with similar actions.

In Tables I–III $v_{1i} = v_{2i} = v_{3i} = v_{9i} = v_{11i}$, $v_{4i} = v_{5i} = v_{6i}$ and $v_{7i} = v_{8i} = v_{10i}$ for $i = t, p$, with the notations

$$\Upsilon_0 = 8\mathrm{Li}_2\left(\frac{3}{4}\right) - \pi^2 + \log\left(\frac{4}{3}\right)(6 - 26\log(2) + 21\log(3)),$$

$$v_{1t} = 3\left(-4\left(\mathrm{Li}_2\left(\frac{1}{4}\right) + \mathrm{Li}_2\left(\frac{1}{3}\right)\right) - 3\log(3)(2 + \log(243))\right.$$
$$\left. + 4\log(2)(3 + 28\coth^{-1}(5))\right) + \pi^2,$$

$$v_{1p} = 1 + 2\log\left(\frac{4}{3}\right)(-5 + 24\log(2) - 12\log(3)),$$

$$v_{4t} = -32\mathrm{Li}_2\left(\frac{1}{4}\right) + 12\mathrm{Li}_2\left(\frac{2}{3}\right) - \frac{10\pi^2}{3} + 7\log^2(3)$$
$$- 54\log(3) + 4\log(2)(23 - 7\log(2) + \log(81)),$$

$$v_{4p} = -96\mathrm{Li}_2\left(\frac{1}{4}\right) + 96\mathrm{Li}_2\left(\frac{1}{3}\right) + 5 + 384\log^2(2)$$
$$+ 4\log(3)(89 + 24\log(3)) - 8\log(2)(73 + 48\log(3)),$$

TABLE I. Diagrams contributing to Z_0. The diagrams are depicted in the second column. In the third column the symmetry coefficients (s.c) are quoted. In the fourth column values of the pole parts of the diagrams are quoted in the normalization of propagators and vertices corresponding to the basic action.

No.	Diagram	s.c	Z_0
1		1	$-\frac{\Upsilon_0}{1536\pi^6\varepsilon}ig_1^2g_2$
2		1	$\frac{\Upsilon_0}{1536\pi^6\varepsilon}ig_1g_2^2$
3		$\frac{1}{2}$	$\frac{\Upsilon_0}{1536\pi^6\varepsilon}ig_1g_2^2$
4		1	$-\frac{\Upsilon_0}{1536\pi^6\varepsilon}ig_1^2g_2$
5		$\frac{1}{2}$	$-\frac{\Upsilon_0}{1536\pi^6\varepsilon}ig_1^2g_2$
6		1	$\frac{\Upsilon_0}{1536\pi^6\varepsilon}ig_2^2g_1$

TABLE II. Diagrams contributing to Z_1 and Z_2. The diagrams are depicted in the second column. In the third column the symmetry coefficients (s.c) are quoted. In the fourth column values of the pole parts of the diagrams are quoted in the normalization of propagators and vertices corresponding to the basic action. In the fifth column the pole parts of diagram derivatives with respect to u at $u = 0$ are presented.

No.	Diagram	s.c	Z_i	$\partial_u Z_i(u=0)$
1		1	$Z_1: \frac{v_{1t}}{9216\pi^6\varepsilon}ig_1^3$	$-\frac{\chi_{1t}}{9216\pi^6\varepsilon}g_1^3$
			$Z_2: -\frac{v_{1p}}{18432\pi^6\varepsilon}ig_1^3$	$-\frac{\chi_{1p}}{110592\pi^6\varepsilon}g_1^3$
2		1	$Z_1: -\frac{v_{2t}}{36864\pi^6\varepsilon}ig_1^2g_2$	$-\frac{\chi_{2t}}{18432\pi^6\varepsilon}g_1^2g_2$
			$Z_2: \frac{v_{2p}}{18432\pi^6\varepsilon}ig_1^2g_2$	$-\frac{\chi_{2p}}{221184\pi^6\varepsilon}g_1^2g_2$
3		1	$Z_1: \frac{v_{3t}}{9216\pi^6\varepsilon}ig_1g_2^2$	$\frac{\chi_{3t}}{9216\pi^6\varepsilon}g_1g_2^2$
			$Z_2: -\frac{v_{3p}}{18432\pi^6\varepsilon}ig_1g_2^2$	$\frac{\chi_{3p}}{27648\pi^6\varepsilon}g_1g_2^2$
4		1	$Z_1: \frac{v_{4t}}{6144\pi^6\varepsilon}ig_1^3$	$\frac{\chi_{4t}}{9216\pi^6\varepsilon}g_1^3$
			$Z_2: \frac{v_{4p}}{36864\pi^6\varepsilon}ig_1^3$	$\frac{\chi_{4p}}{221184\pi^6\varepsilon}g_1^3$
5		$\frac{1}{2}$	$Z_1: -\frac{v_{5t}}{18432\pi^6\varepsilon}ig_1^2g_2$	$-\frac{\chi_{5t}}{18432\pi^6\varepsilon}g_1^2g_2$
			$Z_2: -\frac{v_{5p}}{36864\pi^6\varepsilon}ig_1^2g_2$	$-\frac{\chi_{5p}}{110592\pi^6\varepsilon}g_1^2g_2$
6		1	$Z_1: -\frac{v_{6t}}{18432\pi^6\varepsilon}ig_1^2g_2$	$-\frac{\chi_{6t}}{18432\pi^6\varepsilon}g_1^2g_2$
			$Z_2: -\frac{\chi_{6p}}{36864\pi^6\varepsilon}ig_1^2g_2$	$-\frac{\chi_{6p}}{221184\pi^6\varepsilon}g_1^2g_2$
7		1	$Z_1: -\frac{v_{7t}}{6144\pi^6\varepsilon}ig_1^3$	$-\frac{\chi_{7t}}{9216\pi^6\varepsilon}g_1^3$
			$Z_2: -\frac{v_{7p}}{36864\pi^6\varepsilon}ig_1^3$	$-\frac{\chi_{7p}}{221184\pi^6\varepsilon}g_1^3$
8		1	$Z_1: \frac{v_{8t}}{18432\pi^6\varepsilon}ig_1^2g_2$	$\frac{\chi_{8t}}{9216\pi^6\varepsilon}g_1^2g_2$
			$Z_2: \frac{v_{8p}}{36864\pi^6\varepsilon}ig_1^2g_2$	$\frac{\chi_{8p}}{221184\pi^6\varepsilon}g_1^2g_2$
9		1	$Z_1: -\frac{v_{9t}}{36864\pi^6\varepsilon}ig_1^2g_2$	$-\frac{\chi_{9t}}{9216\pi^6\varepsilon}g_1^2g_2$
			$Z_2: \frac{v_{9p}}{18432\pi^6\varepsilon}ig_1^2g_2$	$-\frac{\chi_{9p}}{221184\pi^6\varepsilon}g_1^2g_2$
10		$\frac{1}{2}$	$Z_1: -\frac{v_{10t}}{36864\pi^6\varepsilon}ig_2^2g_1$	$\frac{\chi_{10t}}{18432\pi^6\varepsilon}g_2^2g_1$
			$Z_2: -\frac{v_{10p}}{36864\pi^6\varepsilon}ig_2^2g_1$	$\frac{\chi_{10p}}{110592\pi^6\varepsilon}g_2^2g_1$
11		1	$Z_1: \frac{v_{11t}}{9216\pi^6\varepsilon}ig_1^3$	$\frac{\chi_{11t}}{9216\pi^6\varepsilon}g_1^3$
			$Z_2: -\frac{v_{11p}}{18432\pi^6\varepsilon}ig_1^3$	$\frac{\chi_{11p}}{110592\pi^6\varepsilon}g_1^3$

$$v_{7t} = 4\left(-2\mathrm{Li}_2\left(\frac{1}{16}\right) + 3\mathrm{Li}_2\left(\frac{1}{9}\right) - 2\mathrm{Li}_2\left(\frac{1}{6}\right)\right.$$
$$+ 5\mathrm{Li}_2\left(\frac{1}{4}\right) + 6\mathrm{Li}_2\left(\frac{3}{8}\right) + 4\mathrm{Li}_2\left(\frac{4}{9}\right) + 3\mathrm{Li}_2\left(\frac{2}{3}\right)\right)$$
$$- \frac{14\pi^2}{3} + 116\log^2(2) - 4\log(2)(17 + 32\log(3))$$
$$+ \log(3)(42 + 47\log(3)),$$
$$\chi_{1t} = -\left(24\mathrm{Li}_2\left(\frac{1}{4}\right) - 84\mathrm{Li}_2\left(\frac{2}{3}\right) - 6 + 7\pi^2\right.$$
$$-576\log^2(2) + 20\log(2)(8 + 33\log(3))$$
$$\left. - \log(3)(80 + 207\log(3))\right),$$

TABLE III. Diagrams contributing to Z_5. The diagrams are depicted in the second column. In the third column the symmetry coefficients (s.c) are quoted. In the fourth column values of the pole parts of the diagrams are quoted in the normalization of propagators and vertices corresponding to the basic action. In the fifth column the pole parts of diagram derivatives with respect to u at $u = 0$ are presented.

No.	Diagram	s.c	Z_5	$\partial_u Z_5(u=0)$
1		$\frac{1}{2}$	$-\frac{3ig_1^3\log\left(\frac{4}{3}\right)}{64\pi^4\varepsilon}$	$-\frac{g_1^3\log\left(\frac{4}{3}\right)}{16\pi^4\varepsilon}$
2		1	$\frac{ig_1^3\left(\log\left(\frac{64}{27}\right)-1\right)}{256\pi^4\varepsilon}$	$\frac{g_1^3(-1+14\log(2)-7\log(3))}{256\pi^4\varepsilon}$
3		1	$\frac{ig_1^3\left(\log\left(\frac{64}{27}\right)-1\right)}{256\pi^4\varepsilon}$	$\frac{g_1^3\left(\log\left(\frac{256}{81}\right)-1\right)}{128\pi^4\varepsilon}$
4		1	$\frac{ig_1^3\left(\log\left(\frac{64}{27}\right)-1\right)}{256\pi^4\varepsilon}$	$\frac{g_1^3(-3+14\log(2)-7\log(3))}{256\pi^4\varepsilon}$
5		1	$-\frac{ig_1^3\log\left(\frac{4}{3}\right)}{64\pi^4\varepsilon}$	$\frac{g_1^3\left(1-6\log\left(\frac{4}{3}\right)\right)}{192\pi^4\varepsilon}$
6		1	$-\frac{ig_1^3\left(1+\log\left(\frac{4}{3}\right)\right)}{256\pi^4\varepsilon}$	$-\frac{g_1^3\left(1+\log\left(\frac{4096}{729}\right)\right)}{384\pi^4\varepsilon}$
7		$\frac{1}{2}$	$-\frac{ig_1^3\left(1+\log\left(\frac{4}{3}\right)\right)}{256\pi^4\varepsilon}$	$-\frac{g_1^3\left(1+\log\left(\frac{4}{3}\right)\right)}{256\pi^4\varepsilon}$
8		1	$\frac{ig_1^3\left(\log\left(\frac{64}{27}\right)-1\right)}{256\pi^4\varepsilon}$	$\frac{g_1^3(-1+14\log(2)-7\log(3))}{256\pi^4\varepsilon}$
9		$\frac{1}{2}$	$\frac{ig_1^3\left(\log\left(\frac{64}{27}\right)-1\right)}{256\pi^4\varepsilon}$	$\frac{g_1^3(-3+14\log(2)-7\log(3))}{256\pi^4\varepsilon}$
10		1	$\frac{ig_1g_2^2\left(\log\left(\frac{64}{27}\right)-1\right)}{256\pi^4\varepsilon}$	$\frac{g_1g_2^2(1-14\log(2)+7\log(3))}{256\pi^4\varepsilon}$

TABLE III. (*Continued.*)

No.	Diagram	s.c	Z_5	$\partial_u Z_5(u=0)$
11		1	$\frac{ig_1g_2^2\left(\log\left(\frac{64}{27}\right)-1\right)}{256\pi^4\varepsilon}$	$-\frac{g_1g_2^2\left(\log\left(\frac{256}{81}\right)-1\right)}{128\pi^4\varepsilon}$
12		$\frac{1}{2}$	$-\frac{ig_1g_2^2\log\left(\frac{4}{3}\right)}{64\pi^4\varepsilon}$	$\frac{g_1g_2^2\left(\log\left(\frac{64}{27}\right)-1\right)}{96\pi^4\varepsilon}$
13		1	$\frac{ig_1^2g_2\left(1+\log\left(\frac{4}{3}\right)\right)}{256\pi^4\varepsilon}$	$\frac{g_1^2g_2\left(\log\left(\frac{64}{27}\right)-1\right)}{768\pi^4\varepsilon}$
14		1	$\frac{ig_1^2g_2\left(1+\log\left(\frac{4}{3}\right)\right)}{256\pi^4\varepsilon}$	$\frac{g_1^2g_2}{384\pi^4\varepsilon}$
15		$\frac{1}{2}$	$-\frac{ig_1^2g_2\left(\log\left(\frac{64}{27}\right)-1\right)}{256\pi^4\varepsilon}$	$\frac{g_1^2g_2\left(\log\left(\frac{1024}{243}\right)-1\right)}{256\pi^4\varepsilon}$
16		$\frac{1}{2}$	$\frac{3ig_1^2g_2\log\left(\frac{4}{3}\right)}{64\pi^4\varepsilon}$	0
17		1	$\frac{3ig_1^2g_2\log\left(\frac{4}{3}\right)}{64\pi^4\varepsilon}$	0
18		1	$-\frac{ig_1^2g_2\left(\log\left(\frac{64}{27}\right)-1\right)}{256\pi^4\varepsilon}$	$\frac{g_1^2g_2\left(\log\left(\frac{16}{9}\right)-1\right)}{128\pi^4\varepsilon}$
19		1	$-\frac{ig_1^2g_2\left(\log\left(\frac{64}{27}\right)-1\right)}{256\pi^4\varepsilon}$	$\frac{g_1^2g_2\left(\log\left(\frac{1024}{243}\right)-1\right)}{256\pi^4\varepsilon}$
20		1	$-\frac{ig_1^2g_2\left(\log\left(\frac{64}{27}\right)-1\right)}{256\pi^4\varepsilon}$	$-\frac{g_1^2g_2\left(\log\left(\frac{16}{9}\right)-1\right)}{128\pi^4\varepsilon}$

TABLE III. (*Continued.*)

No.	Diagram	s.c	Z_5	$\partial_u Z_5(u=0)$
21		$\frac{1}{2}$	$\frac{ig_1^2g_2\left(1+\log\left(\frac{4}{3}\right)\right)}{256\pi^4\varepsilon}$	$-\frac{g_1^2g_2\left(\log\left(\frac{64}{27}\right)-1\right)}{256\pi^4\varepsilon}$
22		1	$-\frac{ig_1^2g_2\left(\log\left(\frac{64}{27}\right)-1\right)}{256\pi^4\varepsilon}$	$-\frac{g_1^2g_2\left(\log\left(\frac{16}{9}\right)-1\right)}{128\pi^4\varepsilon}$
23		$\frac{1}{2}$	$\frac{ig_1^2g_2\log\left(\frac{4}{3}\right)}{64\pi^4\varepsilon}$	0
24		1	$\frac{ig_1g_2^2\left(\log\left(\frac{64}{27}\right)-1\right)}{256\pi^4\varepsilon}$	$-\frac{g_1g_2^2\left(\log\left(\frac{256}{81}\right)-1\right)}{128\pi^4\varepsilon}$

$$\chi_{2t} = -\left(12\mathrm{Li}_2(-2) + 6\mathrm{Li}_2\left(\frac{1}{4}\right) - 6 + \pi^2 - 180\log^2(2)\right.$$
$$\left. + (26 + 96\log(3))\log(4) - (13 + 24\log(3))\log(9)\right),$$

$$\upsilon_{7p} = -192\mathrm{Li}_2\left(\frac{1}{4}\right) + 96\mathrm{Li}_2\left(\frac{1}{3}\right) + 5 - 16\pi^2$$
$$+ 4\log(3)(24\log(3) - 79)$$
$$+ 24\log(2)(21 - 8\log(3) + \log(256)),$$

$$\chi_{3t} = -\left(13\pi^2 - 2\left(-33\mathrm{Li}_2\left(\frac{1}{4}\right) + 78\mathrm{Li}_2\left(\frac{2}{3}\right) + 6\right.\right.$$
$$+ 270\log^2(2) - 4\log(2)(25 + 87\log(3))$$
$$\left.\left. + (25 + 63\log(3))\log(9)\right)\right),$$

$$\chi_{3p} = \left(54\mathrm{Li}_2\left(\frac{1}{4}\right) - 108\mathrm{Li}_2\left(\frac{2}{3}\right) + 15 + 9\pi^2\right.$$
$$+ 972\log^2(2) + \log(3)(113 + 162\log(3))$$
$$\left. - 2\log(2)(113 + 432\log(3))\right),$$

$$\chi_{4t} = -\left(-30\mathrm{Li}_2\left(\frac{1}{9}\right) + 30\mathrm{Li}_2\left(\frac{1}{3}\right)\right.$$
$$- 63\mathrm{Li}_2\left(\frac{3}{4}\right) + 3 + 5\pi^2 - 366\log^2(2) + 97\log(4)$$
$$\left. + \log(3)(-113 - 18\log(3) + 120\log(4))\right),$$

$$\chi_{4p} = \left(-864\mathrm{Li}_2\left(\frac{1}{4}\right) - 3 + 48\pi^2 + 288\log^2(3)\right.$$
$$\left. + 1651\log(9) - 4\log(2)\left(1331 + 864\coth^{-1}(5)\right)\right),$$

$$\chi_{1p} = -\left(216\mathrm{Li}_2\left(\frac{1}{4}\right) - 432\mathrm{Li}_2\left(\frac{2}{3}\right) + 69 + 36\pi^2\right.$$
$$+ 4\log(2)(-221 + 972\log(2) - 864\log(3))$$
$$\left. + 221\log(9) + 324\log(3)\log(9)\right),$$

$$\chi_{5t} = -\left(-18\text{Li}_2\left(\frac{1}{9}\right) + 6\text{Li}_2\left(\frac{1}{4}\right) - 60\text{Li}_2\left(\frac{2}{3}\right) - 12 \right.$$
$$+ 7\pi^2 - 672\log^2(2) + 4\log(2)(37 + 183\log(3))$$
$$\left. - \log(3)(82 + 213\log(3))\right),$$

$$\chi_{5p} = -\left(-9\left(32\text{Li}_2\left(-\frac{1}{3}\right) + 64\text{Li}_2\left(\frac{3}{4}\right) + 1\right) \right.$$
$$+ 48\pi^2 - 6912\log^2(2) + 20\log(2)(173 + 288\log(3))$$
$$\left. - 2\log(3)(1025 + 504\log(3))\right),$$

$$\chi_{6t} = -\left(-126\text{Li}_2\left(\frac{1}{4}\right) - 36\text{Li}_2\left(\frac{1}{3}\right) + 6 + 7\pi^2 \right.$$
$$+ 276\log^2(2) + 36\log^2(3) + 302\log(3)$$
$$\left. - 4\log(2)(119 + 69\log(3))\right),$$

$$\chi_{6p} = \left(-1152\text{Li}_2\left(-\frac{1}{3}\right) - 1440\text{Li}_2\left(\frac{3}{4}\right) + 189 + 96\pi^2 \right.$$
$$- 13248\log^2(2) - 2\log(3)(2381 + 720\log(3))$$
$$\left. + 4\log(2)(1933 + 2592\log(3))\right),$$

$$\chi_{9p} = \left(144\text{Li}_2\left(\frac{1}{4}\right) - 288\text{Li}_2\left(\frac{2}{3}\right) + 57 + 24\pi^2 \right.$$
$$+ 2592\log^2(2) + 432\log^2(3) + 322\log(3)$$
$$\left. - 4\log(2)(161 + 576\log(3))\right),$$

$$\chi_{10t} = \left(6\left(5\text{Li}_2\left(\frac{1}{9}\right) - 10\text{Li}_2\left(\frac{2}{3}\right) + \text{Li}_2\left(\frac{3}{4}\right) + 2\right) \right.$$
$$+ 6\pi^2 + 36\left(\log\left(\frac{16}{9}\right) - 11\right)\log(2)$$
$$\left. + 7(34 - 3\log(3))\log(3)\right),$$

$$\chi_{10p} = (75 - 852\log(2) + 490\log(3)),$$

$$\chi_{11t} = -\left(-6\text{Li}_2\left(\frac{1}{4}\right) - 36\text{Li}_2\left(\frac{1}{3}\right) + 6 + 3\pi^2 + 108\log^2(3) \right.$$
$$\left. + 37\log(9) - 4\log(2)\left(37 + 234\coth^{-1}(5)\right)\right),$$

$$\chi_{7t} = \left(-117\text{Li}_2\left(\frac{1}{4}\right) + 6\text{Li}_2\left(\frac{2}{3}\right) + 3 + \frac{11\pi^2}{2} \right.$$
$$- 90\log^2(2) + (103 - 36\log(3))\log(3)$$
$$\left. + 6\log(2)(14\log(3) - 29)\right),$$

$$\chi_{7p} = -\left(-3\left(-384\text{Li}_2\left(\frac{1}{4}\right) + 192\text{Li}_2\left(\frac{2}{3}\right) + 9 + \log(729)\right) \right.$$
$$\left. + 12\log(2)\left(455 + 16\log\left(\frac{64}{27}\right)\right) - 3352\log(3)\right),$$

$$\chi_{2p} = \left(144\text{Li}_2\left(\frac{1}{4}\right) - 288\text{Li}_2\left(\frac{2}{3}\right) + 57 + 24\pi^2 \right.$$
$$+ 2592\log^2(2) + 432\log^2(3) + 322\log(3)$$
$$\left. - 4\log(2)(161 + 576\log(3))\right),$$

$$\chi_{8t} = -\left(87\text{Li}_2\left(\frac{1}{4}\right) - 18\text{Li}_2\left(\frac{2}{3}\right) + 3 \right.$$
$$- \frac{5\pi^2}{2} - \left(161 + 12\log\left(\frac{8}{3}\right)\right)\log(3)$$
$$\left. + 6\log(2)(43 + \log(512))\right),$$

$$\chi_{8p} = \left(3\left(960\text{Li}_2\left(-\frac{1}{2}\right) - 576\text{Li}_2\left(-\frac{1}{3}\right) \right.\right.$$
$$\left.- 384\text{Li}_2\left(\frac{2}{3}\right) + 89\right) + 192\pi^2$$
$$+ 12(521 - 168\log(2))\log(2)$$
$$\left. + \left(288\log\left(\frac{8}{3}\right) - 2011\right)\log(9)\right),$$

$$\chi_{9t} = -\left(12\text{Li}_2\left(\frac{1}{4}\right) - 24\text{Li}_2\left(\frac{2}{3}\right) - 3 \right.$$
$$+ 2\pi^2 - 72\log^2(2) - \log(3)(13 + 36\log(3))$$
$$\left. + \log(2)(26 + 96\log(3))\right),$$

$$\chi_{11p} = -\left(72\text{Li}_2\left(\frac{1}{4}\right) - 144\text{Li}_2\left(\frac{2}{3}\right) + 3 + 12\pi^2 \right.$$
$$+ 4\log(2)(-65 + 324\log(2) - 288\log(3))$$
$$\left. + 65\log(9) + 108\log(3)\log(9)\right).$$

[1] R. A. Ferrell, N. Menyhárd, H. Schmidt, F. Schwabl, and P. Szépfalusy, Phys. Rev. Lett. **18**, 891 (1967).

[2] B. I. Halperin, Phys. Rev. B **11**, 178 (1975).

[3] M. Suzuki and G. Igarashi, Phys. Lett. A **47**, 361 (1974).

[4] I. Kondor and P. Szepfalusy, Phys. Lett. A **47**, 393 (1974).

[5] A. N. Vasil'ev, *Functional Methods in Quantum Field Theory and Statistical Physics* (Gordon and Breach, New York, 1998).

[6] P. C. Hohenberg and B. I. Halperin, Rev. Mod. Phys. **49**, 435 (1977).

[7] A. N. Vasil'ev, *The Field Theoretic Renormalization Group in Critical Behavior Theory and Stochastic Dynamics* (CRC, Boca Raton, FL, 2004).

[8] M. Dančo, M. Hnatič, M. V. Komarova, T. Lučivjanský, and M. Y. Nalimov, Phys. Rev. E **93**, 012109 (2016).

[9] M. V. Komarova, D. M. Krasnov, and M. Y. Nalimov, Theor. Math. Phys. **169**, 1441 (2011).

[10] M. Dančo, M. Hnatič, M. V. Komarova, T. Lučivjanský, and M. Y. Nalimov, Acta Phys. Pol. A **131**, 651 (2017).

[11] M. Dančo, M. Hnatič, T. Lučivjanský, and L. Mižišin, Phys. Rev. E **102**, 022118 (2020).

[12] Y. A. Zhavoronkov, M. V. Komarova, Y. G. Molotkov, M. Y. Nalimov, and J. Honkonen, Theor. Math. Phys. **200**, 1237 (2019).

[13] M. Hnatich, M. V. Komarova, and M. Y. Nalimov, Theor. Math. Phys. **175**, 779 (2013).

[14] J. Honkonen, M. V. Komarova, Y. G. Molotkov, and M. Y. Nalimov, Nucl. Phys. B **939**, 105 (2019).

[15] J. Honkonen, M. V. Komarova, Y. G. Molotkov, and M. Y. Nalimov, Theor. Math. Phys. **200**, 1360 (2019).

[16] J. Honkonen, M. V. Komarova, Y. G. Molotkov, M. Y. Nalimov, and Y. A. Zhavoronkov, EPJ Web Conf. **226**, 01005 (2020).

[17] T. Altherr and D. Seibert, Phys. Lett. B **333**, 149 (1994).

[18] H.-P. Breuer and F. Petruzzione, *The Theory of Open Quantum Systems* (Oxford University, New York, 2002).

[19] L. M. Sieberer, S. D. Huber, E. Altman, and S. Diehl, Phys. Rev. Lett. **110**, 195301 (2013).

[20] U. C. Täuber and S. Diehl, Phys. Rev. X **4**, 021010 (2014).

[21] R. Folk and G. Moser, J. Phys. A: Math. Gen. **39**, R207 (2006).

[22] N. V. Antonov and A. N. Vasil'ev, Theor. Math. Phys. **60**, 671 (1984).

[23] J. Schwinger, J. Math. Phys. **2**, 407 (1961).

[24] L. V. Keldysh, Sov. Phys. JETP **20**, 1018 (1965).

[25] E. M. Lifshitz and L. P. Pitaevskii, *Statistical Physics. Part 2: Theory of the Condensed State* (Pergamon, New York, 1980).

[26] A. Kamenev, *Field Theory of Non-Equilibrium Systems* (Cambridge University, New York, 2011).

[27] L. T. Adzhemyan, E. V. Ivanova, M. V. Kompaniets, and S. Y. Vorobyeva, J. Phys. A: Math. Theor. **51**, 155003 (2018).

[28] C. De Dominicis, J. Phys. Colloques **37**, C1-247 (1976).

[29] H. K. Janssen, Z. Phys. B **23**, 377 (1976).

[30] J. Honkonen, M. V. Komarova, and M. Y. Nalimov, Nucl. Phys. B **707**, 493 (2005).

[31] J. Honkonen, M. V. Komarova, and M. Y. Nalimov, Nucl. Phys. B **714**, 292 (2005).

[32] J. C. Le Guillou and J. Zinn-Justin, Phys. Rev. B **21**, 3976 (1980).

[33] J. Zinn-Justin, *Quantum Field Theory and Critical Phenomena* (Oxford University, New York, 2002).

[34] M. Y. Nalimov, V. A. Sergeev, and L. Sladkoff, Theor. Math. Phys. **159**, 499 (2009).

[35] C. De Dominicis and L. Peliti, Phys. Rev. Lett. **38**, 505 (1977).

[36] C. De Dominicis and L. Peliti, Phys. Rev. B **18**, 353 (1978).

[37] L. Peliti, in *Dynamical Critical Phenomena and Related Topics*, edited by C. P. Enz, Lecture Notes in Physics (Springer, New York, 1979), Vol. 104, p. 189.

[38] L. Ts. Adzhemyan, M. Danco, M. Hnatic, E. V. Ivanova, and M. V. Kompaniets, EPJ Web Conf. **108**, 02004 (2016).